Optics Communications 282 (2009) 2495–2501

Contents lists available at ScienceDirect

Optics Communications

journal homepage: www.elsevier.com/locate/optcom

Depth of focus extended microscope configuration for imaging of incorporated groups of molecules, DNA constructs and clusters inside bacterial cells

Tomas Fessl [a,b], Shai Ben-Yaish [c], Frantisek Vacha [a,b,d], Frantisek Adamec [b,d], Zeev Zalevsky [c,*]

[a] Faculty of Science, University of South Bohemia, Branisovska 31, 37005 Ceske Budejovice, Czech Republic
[b] Biology Centre of Academy of Sciences, Branisovska 31, 37005 Ceske Budejovice, Czech Republic
[c] School of Engineering, Bar Ilan University, Bar Ilan, Ramat Gan 52900, Israel
[d] Institute of Physical Biology, University of South Bohemia, Zamek 136, 37333 Nove Hrady, Czech Republic

ARTICLE INFO

Article history:
Received 13 September 2008
Received in revised form 17 February 2009
Accepted 18 March 2009

Keywords:
Fourier transform optics
Optical sensing

ABSTRACT

Imaging of small objects such as single molecules, DNA clusters and single bacterial cells is problematic not only due to the lateral resolution that is obtainable in currently existing microscopy but also, and as much fundamentally limiting, due to the lack of sufficient axial depth of focus to have the full object focused simultaneously. Extension in depth of focus is helpful also for single molecule steady state FRET measurements. In this technique it is crucial to obtain data from many well focused molecules, which are often located in different axial depths.

In this paper we present the implementation of an all-optical and a real time technique of extension in the depth of focus that may be incorporated in any high NA microscope system and to be used for the above mentioned applications. We demonstrate experimentally how after the integration of special optical element in high NA 100× objective lens of a single molecule imaging microscope system, the depth of focus is significantly improved while maintaining the same lateral resolution in imaging applications of incorporated groups of molecules, DNA constructs and clusters inside bacterial cells.

1. Introduction

In recent years the topic of lateral super resolution has become an important direction of research while large variety of approaches were developed and deployed in different imaging systems [1]. One of the aspects of improving the resolution capabilities of an imaging system is related to the axial rather than the lateral dimension. Having the object larger than the depth of focus extent provided by the imager, will generate lateral blurring and loss of spatial frequencies and features.

Different approaches were developed during the years to extend the depth of focus of imaging systems. Some are a combination of special optical element that codes the aperture plane of the imaging lens and a digital post processing algorithm [2–5], some are related to aperture apodization by absorptive mask [6–10] and others include the usage of a diffraction optical phase elements such as multi focal lenses or elements with spatially dense distributions [11–13]. Other interesting approaches included tailoring the modulation transfer functions with high focal depth [14] and usage of logarithmic asphere lenses [15].

One interesting approach of extended depth of focus (EDOF) was presented in Refs. [16,17]. There an all-optical way for realization of the extension was demonstrated by attaching a phase-affecting element. The attached element is constructed from a binary phase pattern with spatially low frequency transitions that codes the entrance pupil of the lens. The presented approach had several important features: since this optical element contains low spatial frequencies, it is not sensitive to chromatic aberrations and dispersion (as other diffractive optical elements do) and it has high energetic efficiency not only in the element plane but rather in the object plane. In addition its fabrication is simple and cheap and thus its possible integration into an objective lens. The optical element has high energetic efficiency of close to 100% since it is a phase only element and thus it does not cause apodization by absorptive mask and in addition the phase element has no spatial high frequencies and thus there is no energy loss due to diffraction orders directing energy outside the region of interest.

In this EDOF technology the extension in the depth of focus was obtained by interference of the energy sent by the various parts of the lens aperture to the region of interest.

This all-optical technology was demonstrated also for ophthalmic applications [18] and proved to show improved performance in extending the depth of focus.

* Corresponding author. Tel.: +972 3 5317055; fax: 972 3 7384051.
E-mail address: zalevsz@eng.biu.ac.il (Z. Zalevsky).

0030-4018/$ - see front matter © 2009 Elsevier B.V. All rights reserved.
doi:10.1016/j.optcom.2009.03.044

In this paper we design and realize the concept of Refs. [16,17] for microscopy applications related to imaging of small structures such single molecules [19], DNA clusters and biological cells. In those applications the spatial features are very small and thus the natural depth of focus of the imaging objective is very short. This causes two undesired effects: several objects positioned one near the other cannot be focused simultaneously and single object also has blurred lateral regions because its 3D structure that sometimes extends beyond the depth of focus provided by the imaging system.

Since the proposed all-optical EDOF technology can allow real time extension of focus without energetic losses nor damage to the color fidelity we used the proposed concept for generating an optical binary phase only element that is added to the objective lens of special microscope configuration that is used for imaging applications of single molecules and small biological structures.

The novelty and the goals of this paper are as follows:

- To design and to construct an integrated 100× objective lens with high NA (of 0.95) that provides not only high transversal resolution but also increased depth of focus.
- The optical element that we aim to add to the lens should not increase its aberrations (such as chromatic aberrations) to avoid reduction in the transversal resolution.
- To incorporate this new lens into special microscope system allowing the imaging of group of single molecules, incorporated DNA constructs and clusters inside bacterial cells.
- Due to the application we are aiming for, the energetic efficiency is very important. Therefore, the extension in depth of focus and the improvement of the resolution should not reduce the efficiency of the energetic transmission of the constructed microscope system.
- To demonstrate experimentally that indeed the new lens design provides improved imaging performance for the above mentioned applications, in real time (e.g. in vivo) and in an all-optical way (without digital processing or without usage of a computer or a screen in the loop) such that human observer could see the outcome through the ocular lens of the microscope.

To the best of our knowledge the construction and the experimental demonstration of this special microscope configuration aiming to image very small objects such as group of single molecules, incorporated DNA constructs and clusters inside bacterial cells and having integrated high resolution objective lens with significantly increased depth of focus that improves the imaging performance for such small objects, has not been realized before.

Note that the new optical design of the objective lens used the basic concept of Ref. [17] as the starting working point but then an iterative simulated annealing optimization algorithm was applied in which the constrain of preserving all the spatial frequencies in the MTF plane obtained stronger emphasis, i.e. we took the working point coming from the analytical solution of Ref. [17] and applied simulated annealing optimization on it to optimize our trade-offs which are related to the spectral contrast of the various frequencies versus the focus extension. The parameters that were varied in the simulated annealing process were the diameter of the annular phase mask disc as well as the value of its phase.

In Section 2 we perform the numerical design of the element adapted to the parameters of our microscope configuration. In Section 3 we present the constructed experimental system and the obtained experimental results. The paper is concluded in Section 4.

2. Extension in depth of focus

The mathematical formulation used in Ref. [17] includes defining mathematically a binary phase only element positioned on the exit pupil of an imaging lens. In this case the Optical Transfer Function (OTF) which is the auto correlation of the Coherence Transfer Function (CTF) equals to:

$$H(\mu;Z_i)=\frac{\int_{-\infty}^{\infty}P\left(x+\frac{\lambda Z_i\mu}{2}\right)\sum_{n=1}^{N}\exp\left(ia_n rect\left(\frac{x+\frac{\lambda Z_i\mu}{2}-n\Delta x}{\Delta x}\right)\right)P^*\left(x-\frac{\lambda Z_i\mu}{2}\right)\sum_{n=1}^{N}\exp\left(-ia_n rect\left(\frac{x-\frac{\lambda Z_i\mu}{2}-n\Delta x}{\Delta x}\right)\right)dx}{\int_{-\infty}^{\infty}|P(x)|^2dx} \quad (1)$$

where a_n are binary coefficients equal either to zero or to a certain phase modulation depth: $a_n=(0,\Delta\phi)$ of the phase only element that we design. $\Delta\phi$ is the phase depth of modulation. Δx represents the spatial segments of the element. λ is the wavelength and μ is the coordinate of the OTF plane. P is the aperture of the lens having coordinates of x (the plane of the CTF) and Z_i is the distance between the imaging lens and the sensor. Since we do not want to create a diffractive optical element, i.e. spatially high frequencies (such that there will be no wavelength dependence and no chromatic aberrations) we force $\Delta x \gg \lambda$.

We impose mathematical constrain that the expression of Eq. (1) will have maximal value for the minimal contrasts defined by the OTF within a predetermined range of spatial frequencies. The result obtained in Ref. [17] was of an annular like disc structure with phase $\Delta\phi$ of close to $\pi/2$ (for the green wavelength of 532 nm). The annular like binary phase disc had external dimension of 4.1 mm.

The obtained result is understandable since the annular shape phase only element can cancel the sign inversions (by addition of proper phase to the spatial frequencies where the inversion was) of the quadratic phase generated while defocusing. Although in order to cancel the phase inversion one have to add a phase of π, the best solution in this case was the phase of $\pi/2$. The phase of $\pi/2$ was essential since due to the requirement for continues focused region, one had to cancel the inversions while the quadratic phase appeared but also when one was in focus and there was no quadratic phase. Thus $\pi/2$ is the phase that equally contributes when the object is defocused and when it is in focus.

Thus, the mathematical analytical solution after imposing the previously mentioned constrains over Eq. (1) yields an annular like phase shape element with binary phase of approximately $\pi/2$.

We applied this mathematical solution into Zemax software which is often used for lenses designs (we followed the concepts that were extensively described in Refs. [17,18]). In the software we simulated a full microscope system having 100× objective lens of Olympus with NA of 0.95. We assumed that in the microscope imaging system the distance between the lens and the image plane is $Z_i = 250$ mm and between the imaging lens and the object is $Z_o = 2.5$ mm. The focal length of the objective is $F = 2.475247$ mm and its aperture $D = 4.70296$ mm. Thus, the F number is $F_{\#} = F/D = 0.5263$.

In the simulations presented in Fig. 1 we compute the through focus Modulation Transfer Function (MTF) at the imaging plane (after magnification of 100×) for spatial frequency of 8 cycles per mm (i.e. in the object plane this spatial frequency is equivalent to frequency of 800 cycles per mm). From the obtained results

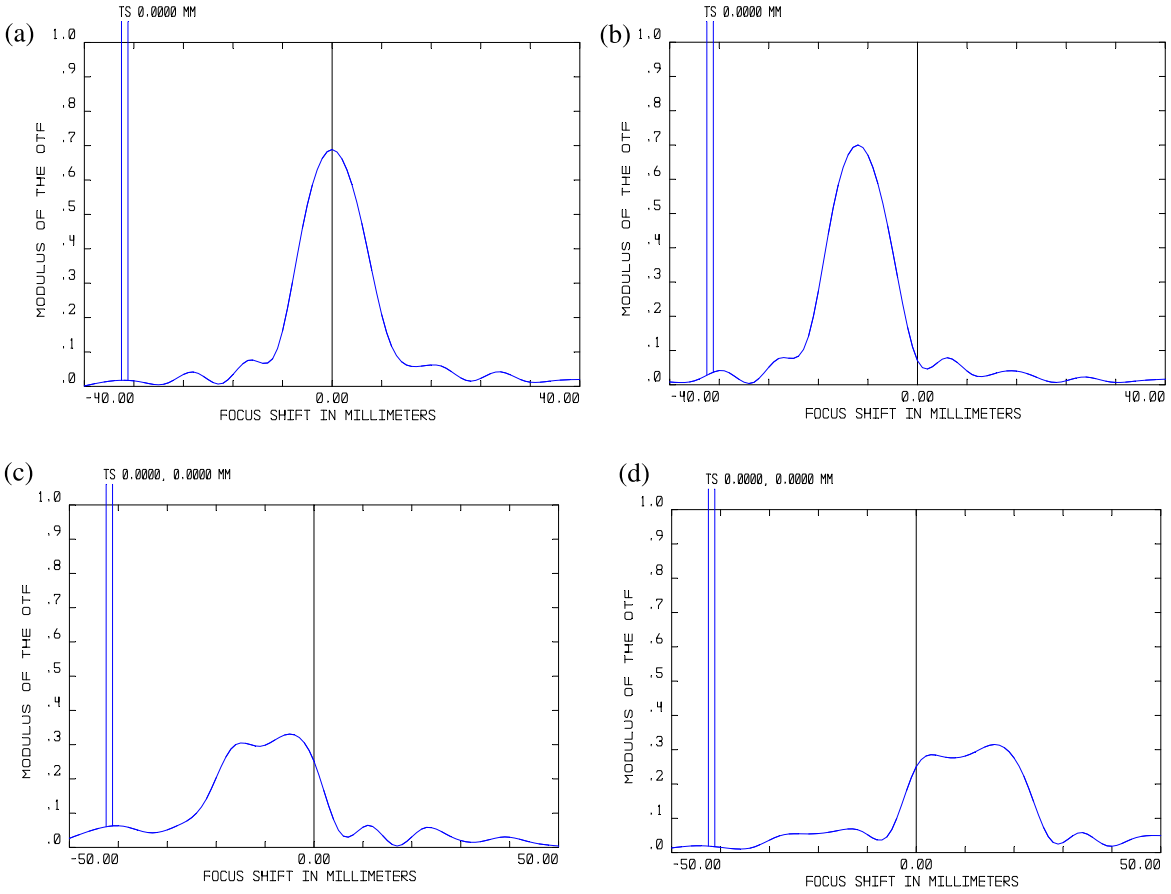

Fig. 1. Numerical simulations of through focus MTF for spatial frequency of 800 cycles/mm (in the object plane). (a) Without EDOF at focus. (b) Without EDOF with shift of +1 μm from focus. (c) With EDOF at position of +1 μm from focus. (d) With EDOF at position of −1 μm from focus.

one may see improvement of at least a factor of 2 in the resulted depth of focus. In Fig. 1a and b we show the through focus MTF without the EDOF element at focus in Fig. 1a and after a shift of +1 μm from the focal position in Fig. 1b. One may see that shift of +1 μm destroyed completely the imaging contrast and resulted with a low pass for the spatial features. Therefore, the overall depth of focus of this objective without the usage of EDOF element is about 1.5 μm (±0.75 μm). When the EDOF element is added one may see that shift of +1 μm (Fig. 1c) or −1 μm (Fig. 1d), from the focal position, preserves the same contrast as obtained while in focus. Therefore, in this case the measurable overall depth of focus is approximately 3 μm (±1.5 μm). The increase of the depth of focus from 1.5 μm into 3 μm in this high resolution microscope can significantly improve the imaging performance for small structures such as a group of single molecules, DNA constructs and clusters inside bacterial cells, since for all of those examples the axial dimension of those objects requires higher depth of focus in order to capture at once their entire structure or in order to see more such structures in-focus in the field of view of the microscope.

From the results of the simulation designs of Fig. 1 one may see that a reduction of about 50% in contrast was obtained. However, please note that this was obtained for a very high spatial frequency of 800 cycles/mm. For a bit lower frequencies lower contrast reduction is obtained and the average reduction in contrast is not that significant (it is less than about 10%). Indeed reduction in signal to noise ratio (SNR) may be compensated by longer integration time and thus one may ask the question of maybe it is simpler just to leave the integration time as is and not to use the EDOF approach and instead increase the axial resolution by mechanical scanning. Regarding this point please note that the reduced SNR is not exactly equivalent to axial scanning. Specifically in the explored application, fast and not static objects are being imaged. Axial scanning will lead to capturing different molecules or other microscopic objects each time because they are constantly moving. There is an advantage of seeing all the axial information at one snap shot while the reduction in the contrast may be compensated by increasing the illumination power and by using a sensor with higher dynamic range or better SNR. This hardware that can compensate the reduction in contrast cannot compensate losing axial resolution.

We have fabricated the designed element using photolithography on SU-8 photo-resist on top of a plastic substrate and added the element, after proper optical alignment, into the experimental setup of the single molecule imaging microscope. Since the phase of this interference element is approximately $\pi/2$, it is very thin (less than 0.3 μm) and can easily be integrated/incorporated into the objective lens of the microscope system.

Please note that if extension in the depth of focus comes on extent of lateral resolution one may as well reduce the NA. However, the point of this paper is exactly to demonstrate the opposite. The proposed approach extends depth of focus WITHOUT loosing lateral resolution and this is why this new improved objective is so suitable for microscopy applications as those explored by this paper. The extension in the depth of focus comes on the extent of some reduction in contrast but not in lose of lateral resolution. This means that the Fourier transform of the point spread function contains all spatial frequencies while some have slightly reduced contrast.

3. Experimental results

The schematic sketch as well as an image (upper right corner) of the microscope system appears in Fig. 2.

The fabricated EDOF element that was designed for this system was positioned attached to the objective lens, aligned and tested with several biological samples.

The microscope configuration consists of: inverted Olympus IX70 microscope, Triax 320 imaging spectrograph with back illuminated liquid nitrogen cooled CCD camera (Spectrum One, Jobin Yvon, 2048 × 512 pixels, pixel size 13.5 × 13.5 μm) and picosecond-pulse laser diode module (PicoQuant LDH-D-C-640, 641 nm, lin. polar) as an excitation source.

We enlarged the objects with objective Olympus 100×, NA of 0.95, UMPLANFL infinity/0, and excited samples with 641 nm by total internal reflection (TIRF).

The microscope is equipped with an Olympus filter cube (Olympus, Japan) containing Raman emitter RS 664 LP (679.3–1497.7 nm), HC-Laser Clean-up MaxDiode 640/8 (Semrock, Germany).

In Fig. 3 we used samples that include a few *E. coli* cells. They are immobilized in a thick layer of polyvinyl alcohol (PVA) (MW 145 000, 98% hydrolyzed, Merck). This places them into different axial depths. There are two transmission images, one with (Fig. 3a) and one without (Fig. 3b) the EDOF element. One may clearly see that when the EDOF element was added more cells are seen in focus.

Inside the *E. coli* cells, there are incorporated double strand labeled oligonucleotides which have 22 base pairs, they are modified by fluorescent label Alexa Fluor 647. Those are incorporated DNA constructs. In Fig. 4 we imaged those samples. Here in contrast to the previous experiments we did not try to position several objects in different axial depths. Nevertheless, even when the objects are in the same plane due to their 3D structure, the usage of the EDOF element significantly improved the axial imaging resolution. The single almost round spots are single molecules. Other shapes on fluorescent images are clusters of constructs, which normally fill the whole bacteria (as could be seen when focusing through the cell). One may clearly see that in Fig. 4a where the EDOF element was used all the clusters are seen due to the extended depth of focus and thus we have an improved axial resolution. In Fig. 4b we did not use the EDOF element and thus the clusters are visible only in the focused part of the *E. coli* cells.

Another example for imaging of small objects is seen in Fig. 5 where a few molecules are incorporated inside the bacterial cell and some others are outside the focal plane. In Fig. 5a where the EDOF element was used much more molecules are seen due to the extended depth of focus and thus improved axial resolution is obtained. In Fig. 5b we did not use the EDOF element and thus much less molecules are visible.

Note that the depth of focus enhancement factor in the experiments validated the numerical designs. The depth of focus exten-

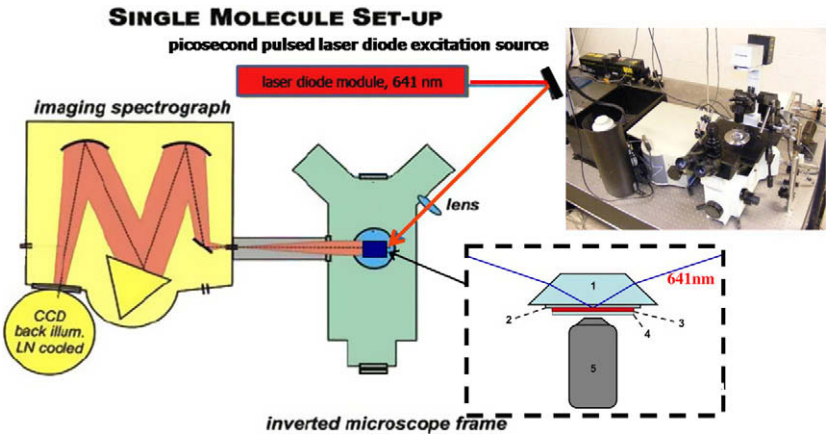

Fig. 2. The experimental setup for single molecule imaging. Item (1) is a quartz TIRF prism, item (2) is quartz cover slip with spin coated layer, item (3) is thin polymer layer with sample, item (4) is the EDOF mask and item (5) is the objective lens.

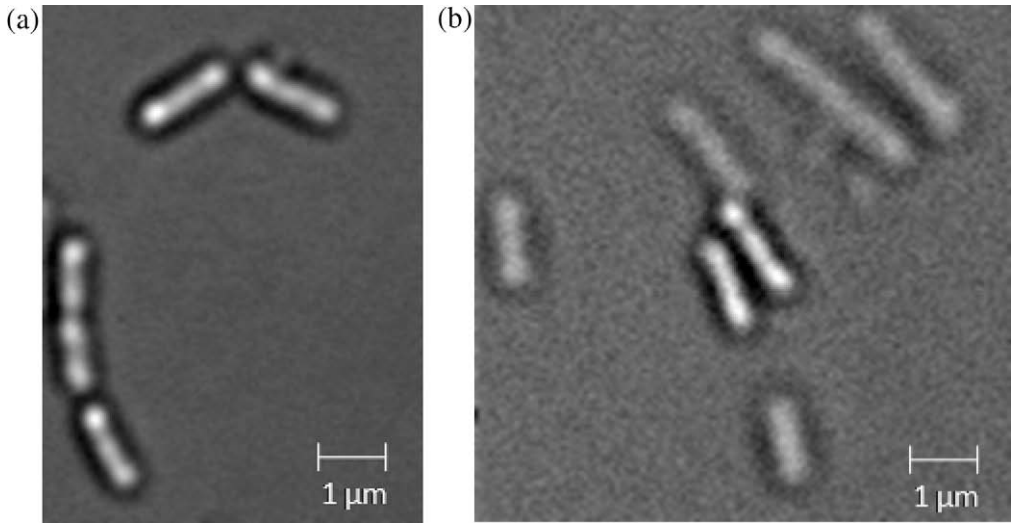

Fig. 3. Samples including a few *E. coli* cells: (a) Transmission image with the EDOF element. (b) Transmission image without the EDOF element.

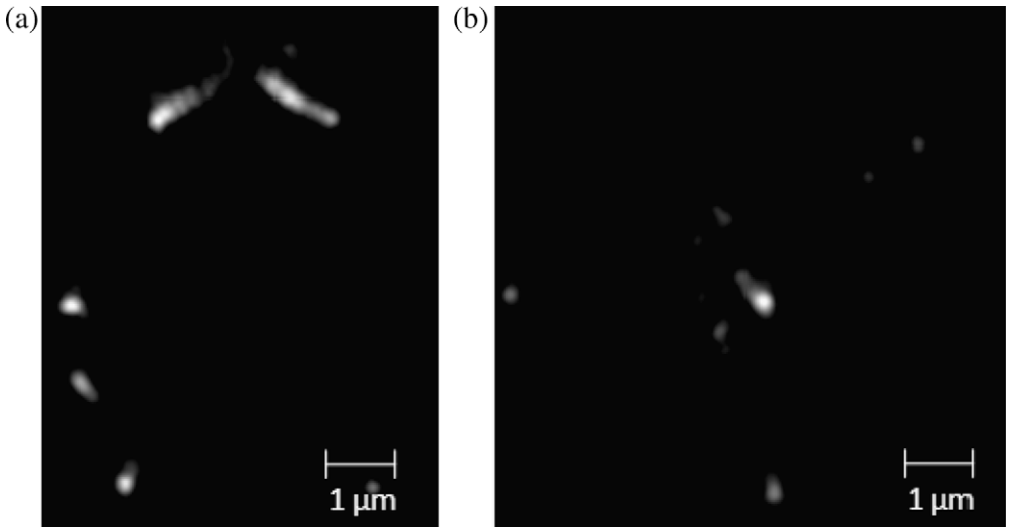

Fig. 4. Imaging of "in cell" incorporated DNA clusters. (a) Fluorescence image of two clusters inside bacterial cell with the EDOF element. (b) Fluorescence image of cluster without the EDOF element.

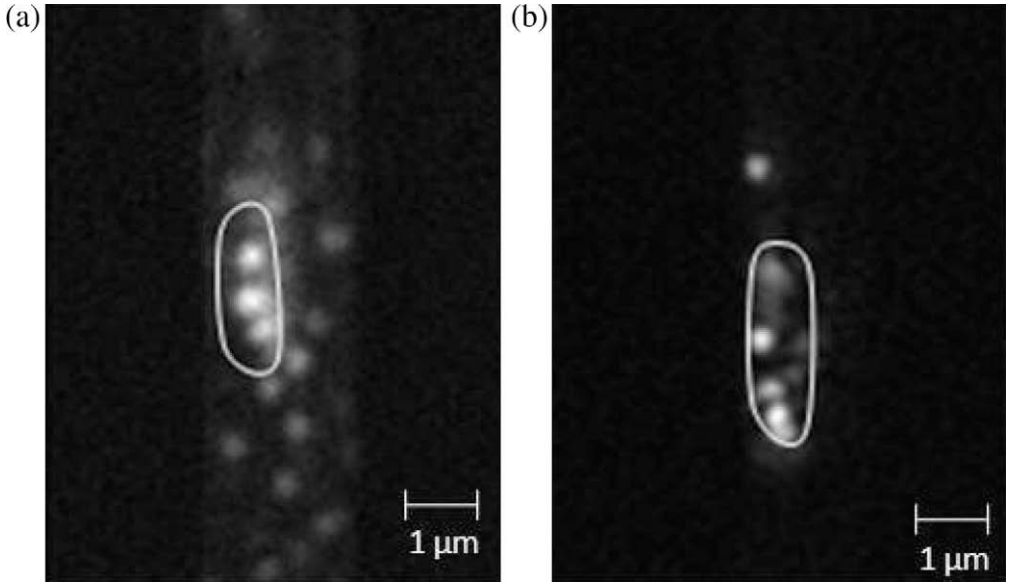

Fig. 5. "In-cell" imaging of few molecules that were incorporated inside the bacterial cell. (a) Fluorescence image with the EDOF element. (b) Fluorescence image without the EDOF element. White line borders the cell shape.

sion factor that was obtained in the experiments was also close to two as obtained in the numerical simulations. Larger extension factor can allow many interesting biological studies such as observing dynamics throughout whole cell body. In our future work we intend to improve the optimization of the EDOF element such that larger extension factors are to be obtained while not as increasing the contrast related compromise.

In further investigation we modified a bit the experimental configuration as it appears in Fig. 6. The microscope configuration consists of: inverted Olympus IX70 microscope, Triax 320 imaging spectrograph with back illuminated liquid nitrogen cooled CCD camera (Spectrum One, Jobin Yvon, 2048 × 512 pixels, pixel size 13.5 × 13.5 μm) and HeCd laser (lin. polarized cw. laser at 442 nm – Kimmon, Japan) as an excitation source. We enlarged the objects with objective Olympus 100×, NA of 0.95, UMPLANFL infinity/0. The microscope is equipped with an Olympus filter cube (Olympus, Japan) containing Razor edge long pass filter 442 nm (Semrock, Germany).

The results from this configuration appear in Figs. 7 and 8.

In Fig. 7 the object was a chlorophyll fluorescence image of moss (Ceratodon purpureus) fragment. Leaves of Ceratodon purpureus were cut into oligocellular linear fragments. Linear chlorophyll containing fragment was fixed in a firm position in the polyvinyl alcohol (PVA) matrix. Due to the tilted position of fragment in the PVA matrix the ends are in different axial depths (the upper-left part of fragment is in focal plane, the down-left part is the most distant visible part). Therefore, we can compare the depth of focus, using the EDOF mask. The object did not move. One may see in Fig. 7a the image obtained without the EDOF mask and in Fig. 7b with the mask. It is easy to see the significant improvement in the depth of focus.

In order to show that the extension in the depth of focus did not reduce the lateral resolution we have captured the images of Fig. 8. The images of Fig. 8 are the transmission image of flake-like crystal structure of PVA. The dark circle in the background is a disc shaped light-shield applied at the condenser side of the cover slide. Due to

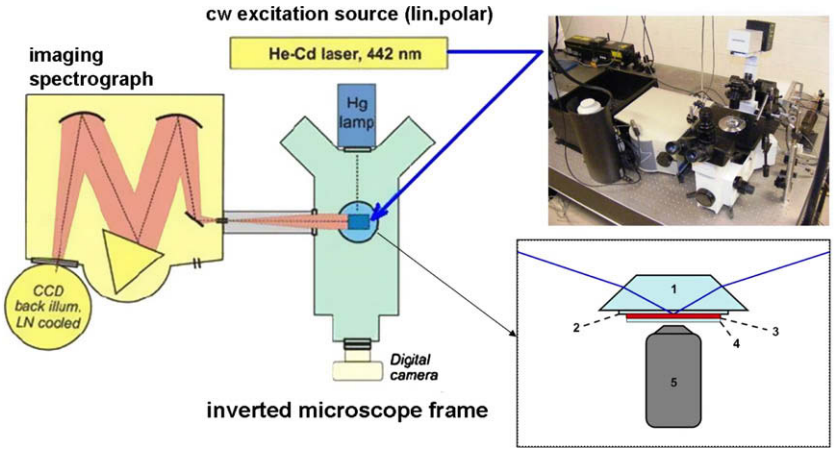

Fig. 6. The schematic sketch and image of the modified experimental setup. Item (1) is a quartz TIRF prism, item (2) is quartz cover slip with spin coated layer, item (3) is thin polymer layer with sample, item (4) is the EDOF mask and item (5) is the objective lens.

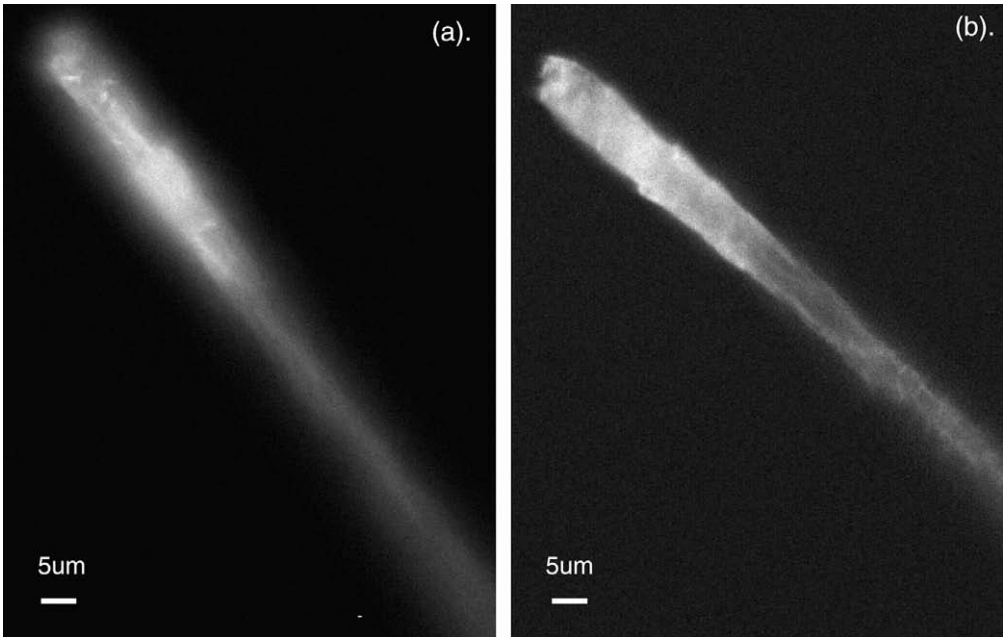

Fig. 7. Chlorophyll fluorescence image of moss (*Ceratodon purpureus*) fragment. (a) Without EDOF mask. (b) With the EDOF mask.

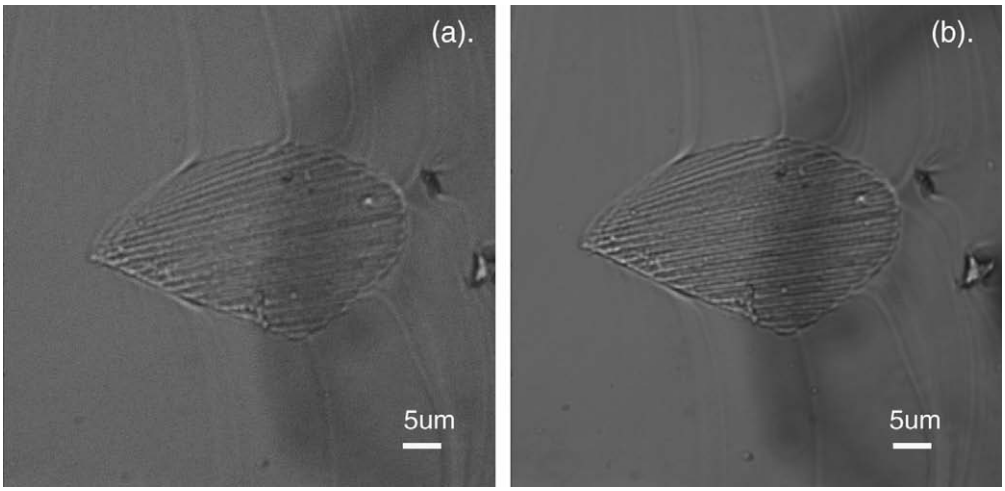

Fig. 8. Transmission image of flake-like crystal structure of PVA. (a) Without EDOF mask. (b) With the EDOF mask.

its fine structure this object can be used as a lateral resolution microscopic target. In Fig. 8a we present the captured image without the EDOF mask and in Fig. 8b it is with the mask. One may see that the lateral resolution is not reduced due to the addition of the EDOF mask.

4. Conclusions

In this paper we have presented the implementation of an all optical approach for extended depth of focus in single molecule imaging microscopy system.

The designed phase only optical element for the extension in depth of focus was fabricated and positioned attaching the objective lens of the microscope. Then, it was experimentally tested in imaging of sub-micron biological samples as incorporated molecules, DNA constructs and clusters inside bacterial cells.

Improved performance of imaging were experimentally demonstrated for plurality of objects positioned in different depths as well as for single small object having 3D structure larger than the existing depth of focus range of the given imaging lens.

Acknowledgments

Zeev Zalevsky acknowledges the support provided to this work by the Israeli Ministry of Science and Technology in grant #1958755.

Tomas Fessl, Frantisek Vacha and Frantisek Adamec acknowledge the financial support by grants GACR202/07/0818, MSM6007665808 and AV0Z50510513.

References

[1] Z. Zalevsky, D. Mendlovic, A.W. Lohmann, Progress in Optics, vol. XL, Chapter 4: "Optical system with improved resolving power", 1999.
[2] W.T. Cathy, E.R Dowski, Apparatus and method for extending depth of field in image projection system, US patent 6069738, May 2000.
[3] W.T. Cathy, Extended depth field optics for human vision, PCT Publication WO 03/052492, June 2003.
[4] E.R. Dowski, W.T. Cathey, Appl. Opt. 34 (1995) 1859.
[5] J. van der Gracht, E. Dowski, M. Taylor, D. Deaver, Opt. Lett. 21 (1996) 919.
[6] C.M. Hammond, Apparatus and method for reducing imaging errors in imaging systems having an extended depth of field, US patent 6097856, August 2000.
[7] D. Miller, E. Blanko, System and method for increasing the depth of focus of the human eye, US patent 6554424, April 2003.
[8] N. Atebara, D. Miller, Masked intraocular lens and method for treating a patient with cataracts, US patent 4955904, September 1990.
[9] J.O. Castaneda, E. Tepichin, A. Diaz, Appl. Opt. 28 (1989) 2666.
[10] J.O. Castaneda, L.R. Berriel-Valdos, Appl. Opt. 29 (1990) 994.
[11] E. Ben-Eliezer, Z. Zalevsky, E. Marom, N. Konforti, D. Mendlovic, All optical extended depth of field imaging system, PCT Publication WO 03/076984, September 2003.
[12] E. Ben-Eliezer, Z. Zalevsky, E. Marom, N. Konforti, J. Opt. A: Pure Appl. Opt. 5 (2003) S164.
[13] E. Ben-Eliezer, E. Marom, N. Konforti, Z. Zalevsky, Appl. Opt. 44 (2005) 2792.
[14] A. Sauceda, J. Ojeda-Castaneda, Opt. Lett. 29 (2004) 560.
[15] W. Chi, N. George, Opt. Lett. 26 (2001) 875.
[16] Z. Zalevsky, Optical method and system for extended depth of focus, US patent No. 7061693 and US patent No. 7365917.
[17] Z. Zalevsky, A. Shemer, A. Zlotnik, E. Ben-Eliezer, E. Marom, Opt. Express 14 (2006) 2631.
[18] Z. Zalevsky, S. Ben Yaish, O. Yehezkel, M. Belkin, Opt. Express 15 (2007) 10790.
[19] G. Chirico, F. Cannone, S. Beretta, G. Baldini, A. Diaspro, Microsc. Res. Tech. 55 (5) (2001) 359.